Characteristics of shallow landslides, soil layer structure and soil properties on hillslopes underlain by granite and hornfels cases from the disaster on 20 August 2014 at Hiroshima, Japan

Takuma WATAKABE[(1)], Yuki MATSUSHI[(2)], Masahiro CHIGIRA[(2)], Ching-Ying TSOU[(2)] and Yasuto HIRATA[(1)]

(1) Graduate school of science, Kyoto University, Japan
E-mail:watakabe@slope.dpri.kyoto-u.ac.jp
(2) Disaster Prevention Research Institute, Kyoto University, Japan

Abstract

In 20 August 2014, a heavy rainstorm triggered more than 450 shallow landslides and debris flows in hillslopes of granite and hornfels in Hiroshima, southwest Japan. The characteristics of landslides differ with geology even they are located under similar rainfall condition (~150 mm/3h). Two types of shallow landsliding emerged in this area; planar translational sliding of soil layer and gush-out failure of gravelly colluvium. Planar sliding occurred both of granite and hornfels and it removed thin soil layer up to 1 m. The mechanism determining the slip depth seems to be different with lithology. Planar sliding in granite form a slip plane at a boundary of mechanical strength in soil profile, while the sliding occurred at hydraulic discontinuity for hillslopes in hornfels area. Gush-out failures were triggered mainly in hornfels area. In many gush-out scars, open-worked gravel layer exposed at the bottom of scar head. This layer may works as conduit for groundwater drainage, however, excess water supply might trigger pore pressure raise, leading to shallow landslide initiations.

Keywords: shallow landslides, granite, hornfels, soil layer structure, soil property

1. Introduction

Rainfall-induced shallow landslides initiate as a result of various subsurface hydrological processes. Major processes triggering shallow landslide are decreasing of effective stress with increasing pore-water pressure. Existence of less-permeable layer in shallow subsurface causes perched water table, leading to buildup of positive pore-water pressure (e.g., Matsushi et al., 2006; Terajima et al., 2014). In some cases, preferential subsurface water flow seems to cause slope instability (e.g. McDonnell, 1990; Dietrich and Dunne, 1993). Pore pressure in soils surrounding preferential flow paths capable to raise when water supply from upslope exceeds drainage capacity of the conduit. Suction loss due to wetting front migration also can trigger soil slip, if weak material composes hillslopes (Matsushi et al., 2006).

Many problems remain unsolved for what factors control location and slip depth of these different types of shallow landslide. Although several previous studies referred to the location prone to form a scar head (e.g. Iida and Okunishi, 1979, Koyama et al., 2005), few studies took into account subsurface hydrological processes (Onda, 1989, Matsushi et al., 2006) and soil layer structure (Wakatsuki et al., 2009, Koyama et al., 2005) which should be related to the occurrence of the different type of shallow landslides, at varying locations and slip depths. Proper slope hazard mitigation requires prediction of location and slip depth for the different type of shallow landslide in hillslopes. Especially, understanding of subsurface vertical profiles of mechanical strength and hydrological properties of soil is essential to discuss initiation processes for each type of landslide.

Different type of shallow landslides occur even under a similar intensity and amount of rainfall when lithological condition set different subsurface structures in hillslopes, as demonstrated in a case of the disaster in August 2014 at Hiroshima, southwest Japan. Landslides occurred with two main types: 1) simple planer soil-layer sliding, and 2) collapse of gravelly colluvium with gush-out of subsurface water forming an outlet of preferential flow paths. The difference in landslide types may reflect varying hydrological processes and mechanical properties owing to different soil layer structures. Surveying these cases in detail, we may be able to reveal the controlling factors of the locations and slip depths of the different types of shallow landslides.

In this study, we categorized types of shallow

landslides for the Hiroshima case on GIS (Geographic Information Systems), and surveyed location of each type of landslide and subsurface hydro-geological structure of slid hillslopes. We selected typical slid hillslopes and carried out geomorphological and geological survey, to find out characteristics in subsurface vertical profiles of mechanical strength and hydrological properties in each type of landslide.

2. Study area

2.1 Geomorphological and geological setting

The study area is hills around Mt. Abu, at northern part of the Hiroshima city (Fig. 1). The major rivers in this area run from northeast to southwest and northwest to southeast forming alluvial low land. The ridgelines of mountains extend northeast–southwest. These geomorphological characteristics reflect the dominant direction of joints originating from past faulting in this area (Takahashi, 1991).

The geology in this area consists of three types of rocks: Jurassic sedimentary rocks, Cretaceous granitic rocks and rhyolite. They are locally intruded by granodiorite porphyry, granite porphyry, and felsite. The sedimentary rocks located around Mt. Abu underwent thermal metamorphism by contact with the surrounding granitic intrusion and changed to hornfels.

The topography in the study area reflects these lithological settings. Granitic areas exhibit a dissected landscape with relatively high valley density and low elevation of mountain peaks, while the area underlain by hornfels forms hill terrain with low valley density and high-relief ridge crest.

The climate in this area is characterized by a template humid condition with mean temperature of 14.8 °C, and average annual rainfall of 1700 mm. Half of the precipitation amount is supplied by frontal activities and typhoons from June to September.

The Hiroshima region has experienced many disasters by landslides induced by heavily rainstorm. Recent severe disaster records are in 1945, 1951, 1967 and 1999 by typhoon and rain fronts (Ushiyama, 2001). In the case of 20 August 2014, a concentrated rain band caused a lot of shallow landslides in the study area, close to the 1999 disaster area.

2.2 Distribution of rainfall amount and shallow landslides in the disaster in 2014

More than 450 shallow landslides occurred in the study area where hillslopes received more than 150 mm of rainfall from 1 to 4 a.m. in 20 August 2014 (Fig. 1).

The landslide density is different by geology. The landslide density is the highest in granite and hornfels.

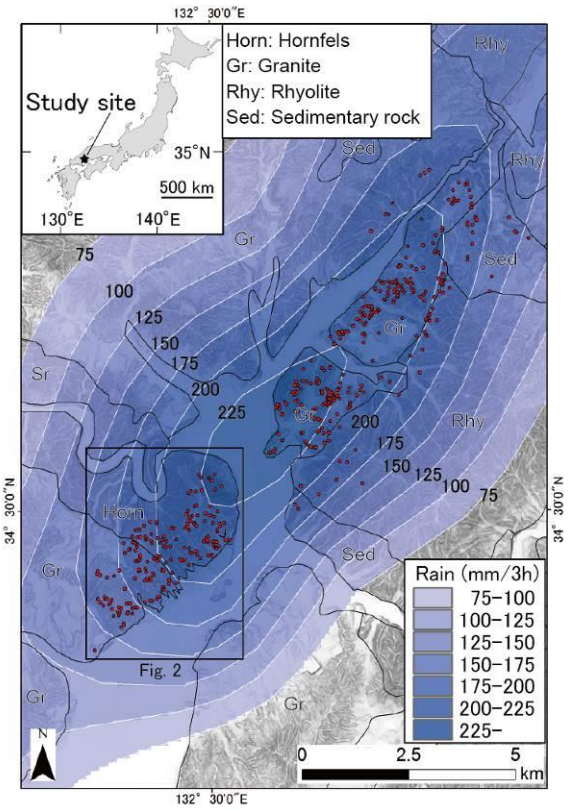

Fig. 1 Topographic and geologic settings around the study area with mapping of rainfall and shallow landslides at the disaster on 20 Aug 2014. Geological boundaries were drawn based on 1/200,000 and 1/50,000 geological maps and topographic analysis by a 1m-mesh digital terrain model (DTM). Red circles indicate source area of shallow landslides. Contours (interval: 25 mm) show rainfall amount from 1 a.m. to 4 a.m on 20 Aug based on records at rain gauges.

Rhyolite and Sedimentary rock areas show much lower density than former two. Therefore, this study focuses hillslopes consists of granite and hornfels (Fig. 2).

Two types of shallow landslides with different shapes emerged in the study area; one is planar sliding and the other is gush-out sliding (Fig. 3). We can distinguish these landslides easily in high-resolution slope-shade map and by field surveys

3. Methods

Detailed geological survey and geomorphological investigation of landslide scars were conducted. Shape of scars, slip depths and lithological conditions are documented in the field. At some landslide scars, we measured longitudinal and cross-sectional profile of landslides with Tru Pulse 360 (Laser Technology Inc.). We categorized the types of shallow landslides based on the field observation linked to topographic

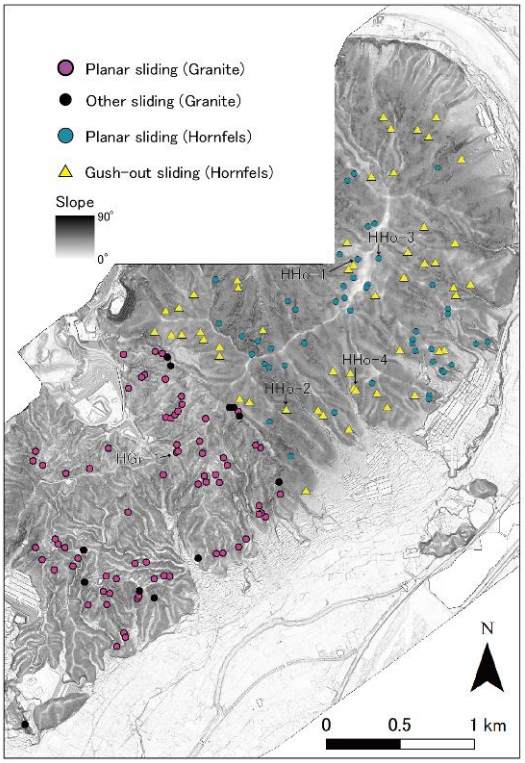

Fig. 2 Slope shade map of the southwestern hills of the landsliding area with mapping of different types of landslide scars. The locations pointed in the map are field observation sites shown in Figs. 3, 5–7.

analysis on GIS, using a LiDAR–derived topographic data and high-resolution ortho photo (Fig. 2, 3).

Two types of shallow landslide are distinguished based on the scar shape and characteristics of material movement; those were 1) planer translational sliding of soil layer, and 2) gush-out failure of gravelly colluvium. Several landslides cannot be categorized to these types since they were induced in relation to geological structure (e.g., wedge failure along geological discontinuity). Each type of landslides were mapped on GIS and analyzed for statistic and topographic aspects of spatial density and distribution.

We selected typical hillslopes with different type of landslide scars to investigate hydro-mechanical soil layer structures. The hillslopes were two planar type slidings for each area of granite and hornfels, and one gush-out failure in the hornfels area. In these slopes, longitudinal profiles were surveyed with 1.5 m–span slope survey tools. Soil soundings were conducted on the profile, using a simplified dynamic cone penetrometer (revised Tsukuba–Maruto Type, with 1.5 cm diameter of 60° cone, knocking by 3 kg weight). The dynamic cone penetration resistance, N_c is defined as knocking numbers needed for a 10 cm penetration of the cone.

To evaluate vertical changes of the soil hydraulic and mechanical properties, we excavated a pit at the scar head to investigate soil layer structure. Potential slip plane were identified on the soil profile. Static

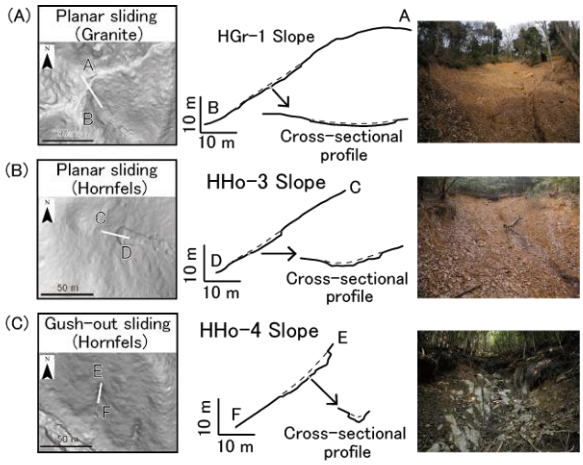

Fig. 3 Shapes of each type of shallow landsliding. (A) Planar sliding in granite. A left image shows the shape of landslide over LiDAR image. A middle figure indicates longitudinal and cross-sectional profile of hillslope. Broken lines indicate paleo-surface. A right picture shows view of sliding. (B) Planar sliding in hornfels. (C) Gush-out sliding in hornfels.

cone penetration test was carried out in-situ on the exposed pit wall by Yamanaka cone penetration tester (Daiki Rika Kogyo Co., Ltd.). Undisturbed soil samples were collected by a 100 cm^3 stainless cylinder at different depths of 10-20 cm intervals. Saturated hydraulic conductivity was measured in lab for the extracted core by the test apparatus (DIK–4012: Daiki Rika Kogyo Co., Ltd.).

4. Results

4.1 Shallow landslide types and density in each geology

Each type of shallow landslides occurred with different spatial frequency with respect to lithological condition. Almost all shallow landslides in the granite area seemed to be categorized to thin (< 1 m thick) planer sliding except for some wedge failure at geological boundary (Fig. 2). In the hornfels area, less than 50% of landslides were planer type (~1 m thick), and more than 50% were gush-out failure of ~3 m thickness of slid material. The total landslide density was almost the same in the granite area (24 scars/km^2) and in the hornfels (25 scars/km^2).

The scars for these different types of landslides emerged at different location. Planer sliding tended to occur at upper hillslopes, while gush-out failure often appeared at lower hillslopes in valley fill. Fig. 4 shows the plot of local gradient against contributing area at the source for each type of landslides. We could not find out distinct separation in gradient but could find a tendency of larger contributing area for the source of gush-out failure in hornfels.

For the gush-out type, open-worked gravel layer was often observed at the bottom of the colluvium exposed at scar head. Subsurface water flowed out

from this conduit just after the disaster occurrence, and we often observed seepage from the layer after it rains during field surveys. This subsurface structure may function for converging subsurface water to slide thick colluvium.

During the field survey, we usually observed a thicker weathering profile in the upper area near main ridge in the hornfels area. The spatial distribution of highly weathered soil layer may control the distribution of the planar sliding in the hornfels area.

4.2 Soil layer structure and vertical change of soil properties

The granite hillslope selected for the detailed survey was characterized by a thick weathering zone in ridge (Fig. 5A). A planar sliding occurred at hillslope with angle about 38° that roughly corresponded to a transition zone from gentle ridge crest to steep slopes. At the sounding point of HGr-1.3, cone penetrometer encountered hard substrates (N_c > 40) at shallow depth, which may correspond to a corestone emerged in the weathering profile. In contrast to the thick weathering material in ridge area, only thin soils remain below the landslide scar.

The potential slip surface for this granite planar sliding was recognized at the depth of 65 cm, at transition between weak colluvial soil and relatively stiff residual dominant soil (Fig. 5B). The changes in mechanical strength were observed in profiles of N_c values and Yamanaka soil hardness (Fig. 5C, D). Below that depth, mechanical strength clearly changed at boundary between soil and saprolite at depth of 80–90 cm. Hydraulic conductivity decreased gradually to 10^{-5} cm/s with increasing depth, but did not show any transition across the slip surface (Fig. 5E).

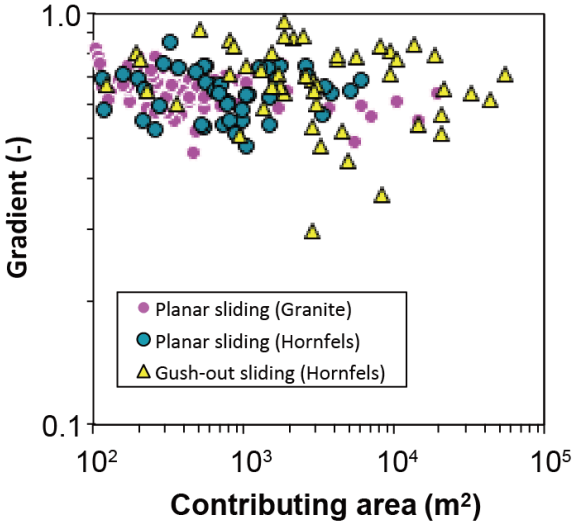

Fig. 4 Gradient vs contributing area. Gradient indicates average value in a part of source area. Contributing area show upward watershed around scar heads.

In the hillslope with planar sliding in the hornfels area (Fig. 6A), hillslope angle down from the flat ridge was uniform around 30° and the bedrock surface was almost parallel to the slope surface with 2 m thickness of soil layer. The landslide slipped almost parallel to the slope remaining ~1 m of weathered material. At the soil-bedrock interface N_c values increased sharply to reach the values of hard unweathered rock.

In the pit at the scar head of planar sliding in hornfels, hard bedrock emerged at the 1.5 m depth, and soil could be classified into colluvial and residual soils according to their color (Fig. 6B). The boundary between reddish brown colluvial soil and light-colored yellowish brown residual soil existed around 90–100 cm deep. This depth accords with the potential slip surface. Yamanaka soil hardness value decreased toward slip surface and increased again to the depth of bedrock (Fig. 6D). Sharp decrease (~1/1000) of hydraulic conductivity observed for the sample extracted at the 90 cm depth (Fig. 6E).

In the hillslope of gush-out failure, colluvial materials of 2–3 m thickness cover the hard bedrock (Fig. 7A). The failure plane corresponded to the hard bedrock surface, which seemed not to parallel to the hillslope. During the sounding survey, N_c value frequently jumped and dropped, and in some cases, it became impossible to penetrate at a shallow depth. This probably due to large gravels trapped in the soil layer supplied by soil creep or past landslides from surrounding hillslopes. A hole with ~50 cm diameter filled with angular cobbles appeared just above the hard bedrock at the scar head of gush-out failure (Fig. 7B). The hydro-mechanical properties of the matrix of the colluvial soil were almost uniform in the 1.5 m profile with weak (N_c < 6 and ~ 19 of Yamanaka hardness) and permeable (K >10^{-5} cm/s) materials (Figs. 7C~E). Below the depth of 150 cm, open-worked gravel layer existed at the bottom of the scar. This layer obviously has a much higher bulk hydraulic conductivity due to the large pore size.

5. Discussion

5.1 Correlation between soil structure and landslide type in granite and hornfels

Slip surface of the planar sliding in the granite hillslope was formed at 65 cm depth, corresponding to the depth of slight increase in mechanical strength (Fig. 5C, D). Dynamic cone penetration resistance shows an uniformly weak values (N_c < 2) at shallower part (0-60 cm), but increases to a slightly larger value (N_c ~5) below 60 cm (Fig. 5C). Static cone penetration hardness also increases from 12 to 17 mm across the depth of potential slip surface. This strength change accords with transition from upper

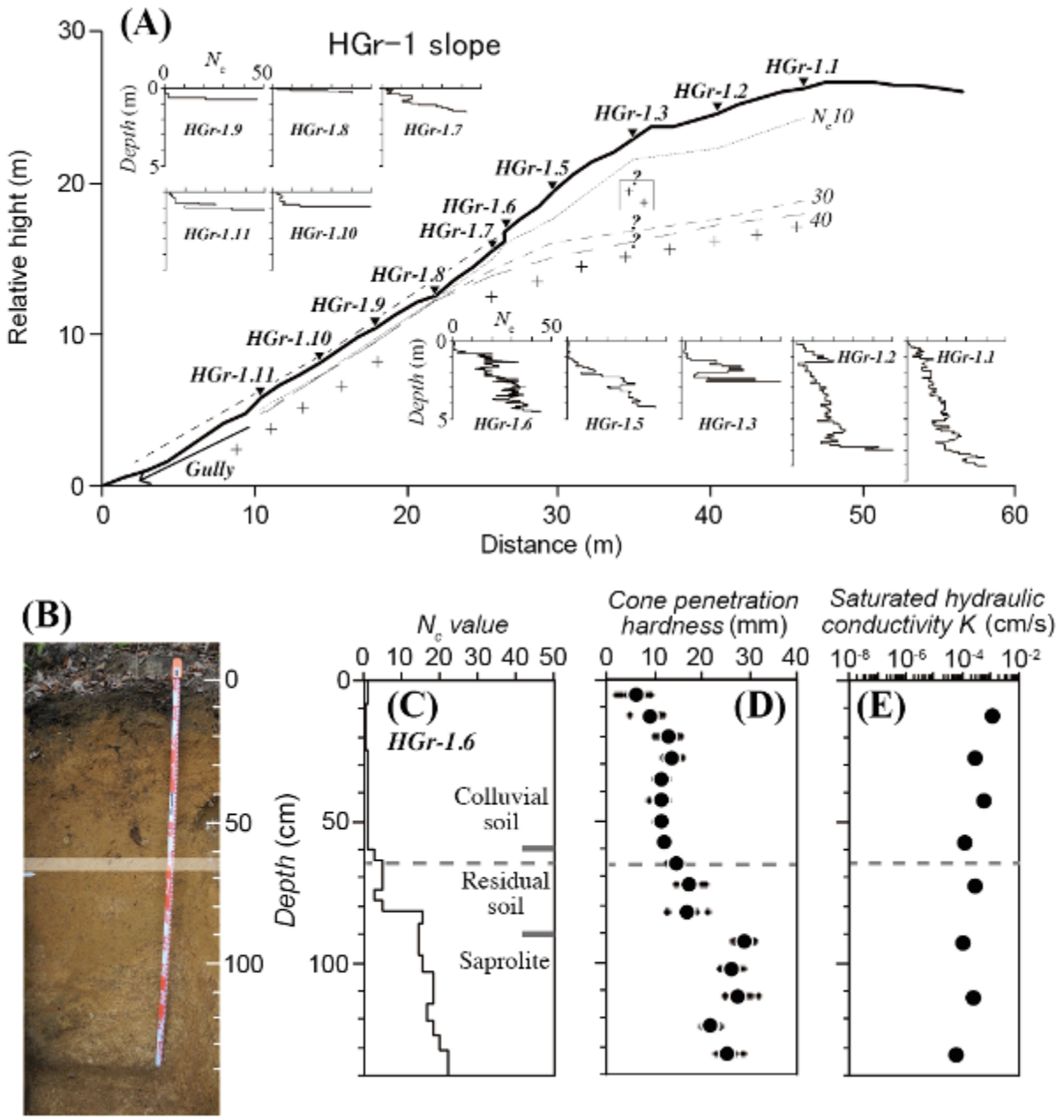

Fig. 5 Soil layer structure and changes of vertical direction of mechanical/hydrological properties in planar sliding in granite. (A) Internal structure of hillslope. N_c 10 and 40 represent weakness layer and bedrock, respectively. Inset graphs show results of dynamic cone penetration sounding. (B) Picture of scar head. White band shows slip surface depth. (C) Results of dynamic cone penetration test at HHr-1.6. Vertical change of soil layer was recognized that 0–65 cm depth is colluvial soil, 65–90 cm is residual soil and 90 cm– saprolite. (D) Results of Yamanaka cone penetration test. Large black circles indicate average value of test. Small black circles show original data. (E) Results of hydraulic conductivity test. Gray broken lines (C,D,E) indicate slip surface depth.

colluvial soil to lower residual material (Fig. 5B). Formation of slip surface at the boundary between soft colluvial and stiff residual layers may control the initiation of planar sliding. Saturated hydraulic conductivity was comparable in these layers in the orders of 10^{-4}–10^{-3} cm/s (Fig. 5E), indicating that both of them are permeable. Koyama et al. (2005) also found fragile layer (N_c < 1) at shallow depths (< 1 m) of hillslopes prone to landsliding in Tottori Pref. near Hiroshima. These findings indicate that existence of discontinuity in mechanical strength play a significant role in the initiation of planer shallow landsliding.

Slip surface of the planar sliding in the hornfels hillslope was formed at a depth of 90–100 cm, corresponding to the hydraulic discontinuity. The upper soil has a higher permeability (saturated hydraulic conductivity K ~ 10^{-6}–10^{-4} cm/s at 15–75

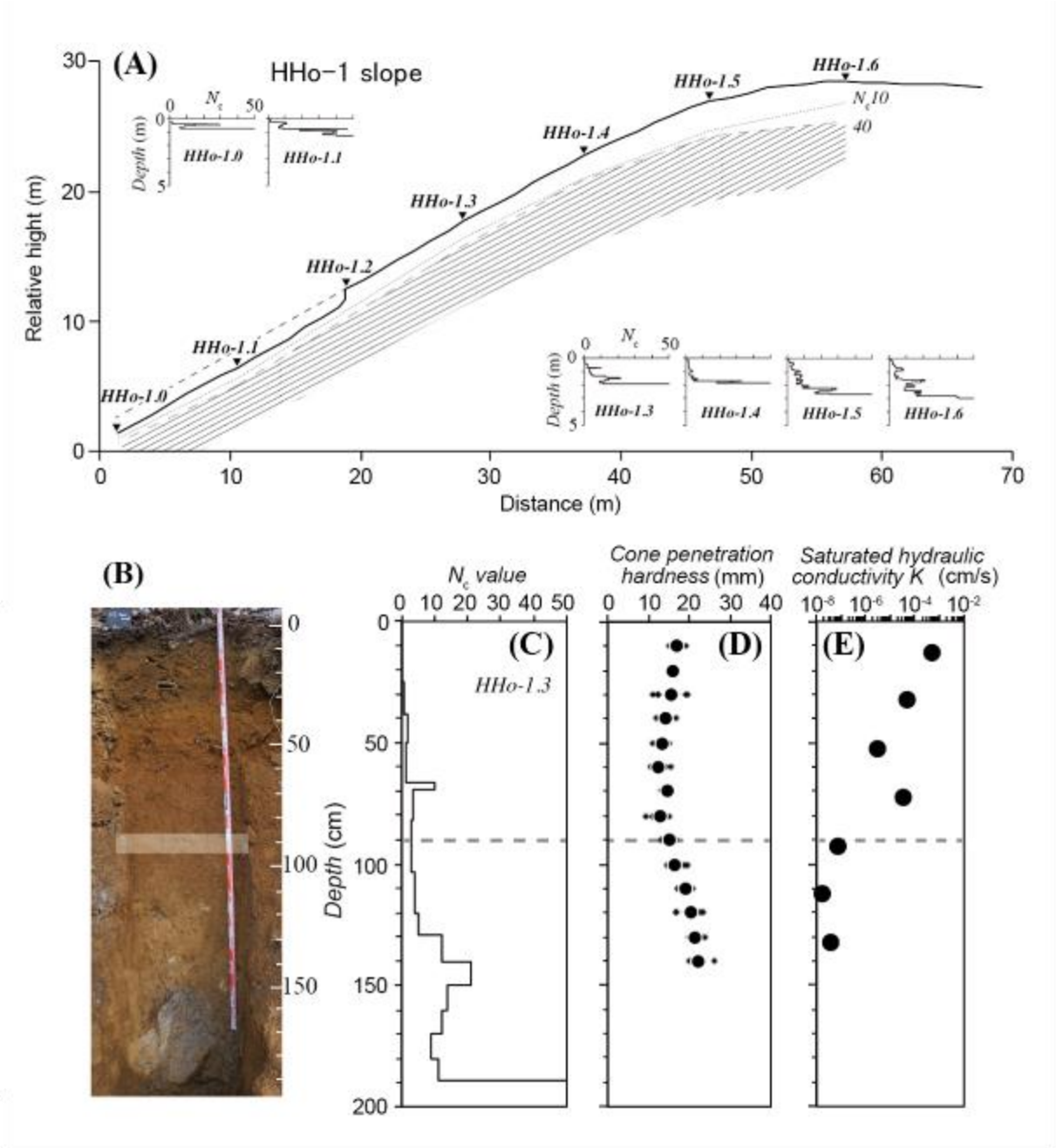

Fig. 6 Soil layer structure and changes of vertical direction of mechanical/hydrological properties in planar sliding in hornfels. Legends are the same in Fig. 5. (A) Internal structure of hillslope. (B) Picture of scar head. (C) Results of dynamic cone penetration test at HHo-1.3. (D) Results of Yamanaka cone penetration test. (E) Results of hydraulic conductivity test.

cm), whereas lower material is less-permeable (K ~ 10^{-8} cm/s) below 90 cm (Fig. 6E). Saturated hydraulic conductivity decreases significantly across the slip surface. This change in permeability accords with transition from reddish-brown upper colluvial soil to lower residual material with color of yellowish light-brown (Fig. 6B). Static cone penetration hardness gradually decreases with increasing depth in the colluvial soil (10–80 cm: from 17 to 13 mm) and gradually increases with depth in the residual material (90–140 cm: from 15 to 22 mm) (Fig. 6D). Dynamic cone penetration resistance (N_c) shows values less than 2 at shallower part (0–67 cm) but increases slightly (N_c ~5) below 70 cm at 10.5 m upslope from the scar head (Fig. 6A, C). Existence of residual material including heavily weathered gravels may contribute to this strength increase. These results imply that hydrological and mechanical discontinuity at the colluvial-residual boundary in the shallow soil layer significantly affects the formation of slip surface. Less-permeable layer may restrict the migration of wetting front to deeper layer and perched water arises as a result of a saturated subsurface water flow in shallow soil layer during heavy rainfall (Matsushi et al. 2006; Wakatsuki et al. 2009; Terajima et al. 2014). Therefore planar shallow

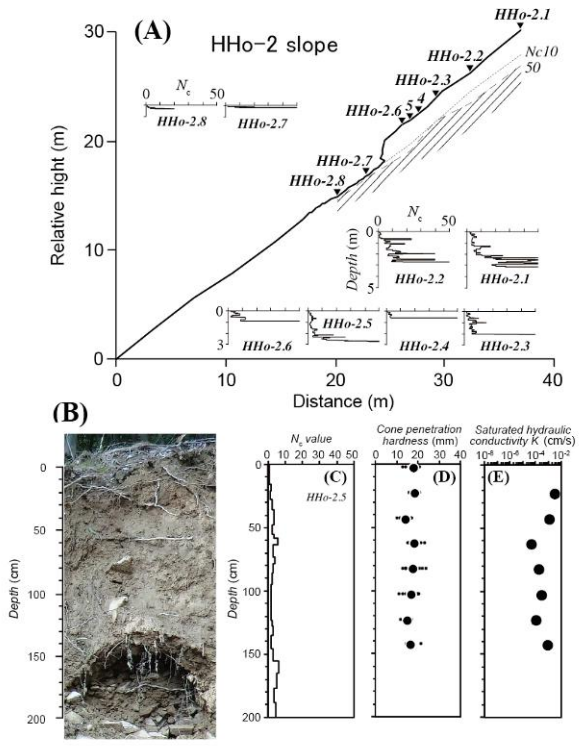

Fig. 7 Soil layer structure and changes of vertical direction of mechanical/hydrological properties in gush-out sliding in hornfels. Legends are the same in Fig. 5. (A) Internal structure of hillslope. (B) Picture of scar heads. (C) Results of dynamic cone penetration test at HHo-2.5. (D) Results of Yamanaka cone penetration test. (E) Results of hydraulic conductivity test.

landsliding in hornfels removed only thin soil layer (~1 m).

Slip surface of the gush-out sliding in the hornfels hillslope was formed at depth of 200 cm along the bottom of open-worked gravel layer (Fig. 7B). Dynamic cone penetration resistance, static cone penetration hardness and saturated hydraulic conductivity show almost uniform value in soil above the gravel layer (Fig. 7C–E). No data was available in depths of the gravel layer (150–200 cm) because of many hard angular gravels and large pores. These characteristic soil structures may originate from colluvial deposits by past landsliding. We can find an old landslide scar at the upper hillslope of this gush-out sliding. This open-worked gravel layer may function as a bypass to transport soil water to downslope. When water infiltration exceeds the drainage ability of the gravel layer, excess pore-pressure should generate, leading to a relatively deep landsliding by slippage of whole soil layer.

5.2 Location of shallow landslide

Most of planar slidings in granite and hornfels occurred at linear part of hillslope, just below a slope break near ridgelines (Figs. 4, 5A, 6A). The location of scar head in granite corresponds to transition zone of hillslope segments covered by thick to thin weathered layers (N_c<40) (Fig. 5A). The difference in thickness of weathered zone indicates upper limit of shallow landslide, and the thin weathered zone results from removal of material by repeated shallow landslides (Iida and Okunishi, 1979).

The spatial distribution of heavily weathered zone and its mechanical and hydraulic properties should affect location of landslide in areas of hornfels. Similar control of landslide location was reported by (Matsuzawa et al. 2014). Shallow landslide could occur in the steep edge of heavily weathered mantle, even the bedrock had been recognized as insusceptible to shallow landsliding. In addition to the topography and thickness of the weathered material, the location of scar head in the hornfels hillslope in the Hiroshima case may be controlled by distance from ridge needed for occurrence of perched water on the less-permeable layer.

Upslope contributing area at most of gush-out sliding (10^2-10^5 m^2) tends to be larger than that of planar slidings up to 10^3 m^2 (Fig. 4). This indicates that gush-out sliding needs a certain amount of water accumulation for failure initiation. The drainage capacity of the open-worked gravel layer may control the location of scar head formation. This hypothesis should be verified by hydrological observations in the valley filling colluvial material in the hornfels area.

6. Conclusions

In this paper, we addressed the question why do shallow landslides due to heavy rainfall differ in their shapes, depths, locations and density on hillslopes underlain by granite and hornfels in northern Hiroshima city. The conclusions are summarized as follows.

(1) In granite hillslopes, most of landslides were planar sliding along mechanical strength discontinuity in soil layer, which corresponds to boundary between colluvial–residual materials.

(2) In hornfels area, planar sliding occupies 50% in number of landslides. Less-permeable residual layer exists beneath colluvial soil layer. This hydraulic discontinuity may form perched water table within the soil layer during the heavy rainfall, leading to planar shallow landsliding.

(3) The other type of landslide in hornfels hillslopes was gush-out sliding. Open-worked gravel layer often outcropped at the bottom of the scar heads. The gush-out landslides may occur when water infiltration flux exceeds drainage ability of the gravel layer.

(4) Gush-out sliding in valley fill tends to have a larger contributing area than the planar slidings near ridgeline. Subsurface water accumulation by lateral

flow may be critical for initiation of the gush-out slidings.

To understand the mechanisms of different types of shallow landslide, we need to evaluate shear strength parameters and soil thickness on hillslopes for slope stability analysis. Measurement of subsurface hydrological processes is also required to reconstruct slope destabilization by rainwater infiltration.

Acknowledgements

The authors are grateful to Aero Asahi Corporation, provided the 1 m–mesh DTM data. This study was supported by the JSPS KAKENHI (26900001, 26702010, 23221009), funding from Natural Disaster Research Council, Disaster Prevention Research Institute, Kyoto University, and from Institute of Sustainability Science, Kyoto University.

References

Dietrich, W. E. and Dunne, T. (1993) Channel head, *In* channel network hydrology. Beven, K. J. and Kirkby, M. J. (eds.). John Wiley and sons, New York, pp. 175-220.

Iida, T. and Okunishi, K. (1979): On the slope development caused by the surface landslides, Geographical Review of Japan. Vol. 52, No. 8, pp. 426-437. (in Japanese with English abstract).

Koyama, K., Sammori, T., Ochiai, H., Okumura, T. and Honda, N. (2005): Influences of fragile layer on surface failure in weathered granite slope, J. Jpn. For. Soc. Vol. 87, pp. 304-312. (in Japanese with English abstract).

Matsushi, Y., Hattanji, T. and Matsukura, Y. (2006) Mechanisms of shallow landslides on soil-mantled hillslopes with permeable and impermeable bedrocks in Boso Peninsula, Japan, Geomorphology, Vol. 76, pp. 92-108.

Matsuzawa, M., Chigira, M., Doshida, S. and Nakamura, T. (2014) Landslide sites controlled by the denudation front and weathering intensity: sallow landslides induced by rainstorms in the area underlain by the Cretaceous Izumi Group, Ehime Prefecture, Jour. Japan Soc. Eng. Geol., Vol. 55, No. 2, pp. 64-76. (in Japanese with English abstract).

McDonnell, J. J. (1990) The influence of micropores on debris flow initiation, Q. J. Eng. Geol. Vol. 23, pp. 325-331.

Onda, Y. (1989): Influence of water storage capacity in regolith zone on runoff characteristics and slope failure on granitic hill in Aichi, Japan, Transactions, Japanese Geomorphological Union. Vol. 10, No. 1, pp. 13-26. (in Japanese with English abstract).

Takahashi, Y. (1991): Geology of the Hiroshima District. With Geological Sheet Map at 1 : 50,000, Geol. Surv. Japan, pp. 1-41. (in Japanese with English abstract)

Terajima, T., Matsushi, Y. and Hattanji, T (2014) Hydrogical aspects to shallow landslide occurrence in Izu-Oshima Island, Triggered by a heaby rainfall of typhoon 20th on October 15-16, 2013, Annuals of Disas. Prev. Res. Inst., Kyoto Univ., Vol. 57A, pp. 17-24. (in Japanese with English abstract)

Ushiyama, Y. (2001): Characteristics of heavy rainfall in Hiroshima city on June 29, 1999, based on precipitation data since 1901, J. JSNDS. Vol. 20, No. 1, pp. 59-74. (in Japanese with English abstract).

Wakatsuki, T., Iida, T., Matsushi, Y., Kogure, T., Sasaki, Y. and Matsukura, Y. (2009): The effect of rock weathering on soil formation and form of slope failure on two mudrock slopes: a case study on slope failures caused by typhoon 10, 2003 in Hidaka District, Hokkaido, Transactions, Japanese Geomorphological Union. Vol. 30, No. 4, pp. 267-288. (in Japanese with English abstract).